

# NJC

Accepted Manuscript



This article can be cited before page numbers have been issued, to do this please use: X. Liang, H. Han, Z. Yan, L. Liu, Y. Zheng, H. Meng and W. Huang, *New J. Chem.*, 2018, DOI: 10.1039/C7NJ04482H.



This is an Accepted Manuscript, which has been through the Royal Society of Chemistry peer review process and has been accepted for publication.

Accepted Manuscripts are published online shortly after acceptance, before technical editing, formatting and proof reading. Using this free service, authors can make their results available to the community, in citable form, before we publish the edited article. We will replace this Accepted Manuscript with the edited and formatted Advance Article as soon as it is available.

You can find more information about Accepted Manuscripts in the [author guidelines](#).

Please note that technical editing may introduce minor changes to the text and/or graphics, which may alter content. The journal's standard [Terms & Conditions](#) and the ethical guidelines, outlined in our [author and reviewer resource centre](#), still apply. In no event shall the Royal Society of Chemistry be held responsible for any errors or omissions in this Accepted Manuscript or any consequences arising from the use of any information it contains.



NJC

Paper

## Versatile functionalization of trifluoromethyl based deep blue thermally activated delayed fluorescence materials for organic light emitting diodes

Received 00th January 20xx,  
Accepted 00th January 20xx

DOI: 10.1039/x0xx00000x

www.rsc.org/

Xiao Liang,<sup>a</sup> Hua-Bo Han,<sup>b</sup> Zhi-Ping Yan,<sup>b</sup> Liang Liu<sup>b</sup>, You-Xuan Zheng<sup>b,\*</sup>, Hong Meng<sup>a,\*</sup>, Wei Huang<sup>a</sup>

Thermally activated delayed fluorescence (TADF) materials have been thoroughly developed and proven to be the most promising means to generate efficient deep blue emission. In this work, we prepared a series of deep blue TADF emitters based on trifluoromethyl featuring phenyl and *N*-heterocyclic rings as electron-withdrawing units and carbazole as electron-donating moieties. Efficient organic light-emitting diodes (OLEDs) utilizing these emitters have deep blue emission and high external quantum efficiency up to 20.4%. These blue emitters are among the bluest in TADF based OLED category. They can also be implemented in OLED as hosts for green phosphorescent iridium(III) complexes, exhibiting high brightness and decent external quantum yield.

### Introduction

The development of organic light-emitting diodes (OLEDs) has been robustly grown since C.W. Tang<sup>1</sup> reported the first generation OLED based on fluorescent emitters. But the traditional fluorescent materials can only harvest the singlet excitons during the electroluminescence process, limiting the theoretical external quantum efficiency to merely 25%.<sup>2</sup> The introduction of heavy metals such as iridium and platinum breaks the limitation due to strong spin-orbit coupling effect, endowing the emitter with the ability to harvest both singlet and triplet excitons<sup>3</sup>, boosting theoretical quantum yield up to 100%.<sup>4</sup> However, the introduction of heavy metals also restricts the potential of developing efficient deep blue emitters<sup>5</sup> and increases the overall cost of OLED. It remains to be a bottleneck for traditional phosphorescent materials until the recent breakthrough with thermally activated delayed fluorescence (TADF) reported by Adachi. et.al<sup>6-9</sup>. The TADF molecules can overcome the demerit of traditional fluorescent materials by recursive energy transfer from  $T_1$  to  $S_1$  due to the small energy gap between  $S_1$  and  $T_1$ , providing a significantly efficient pathway to harvest the triplet energy<sup>10</sup>. Since then, a

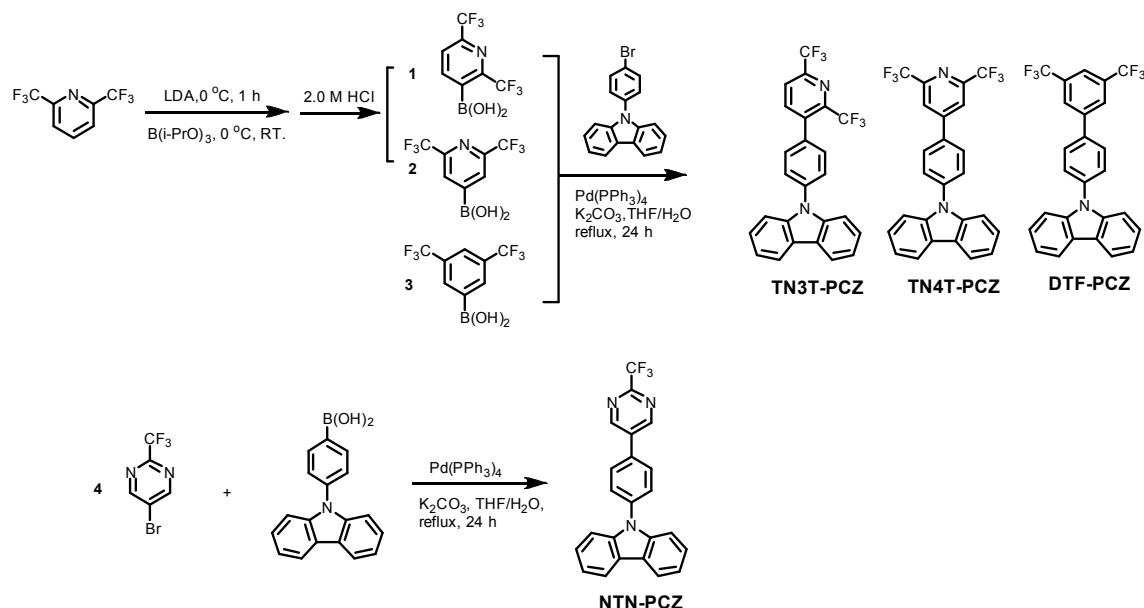
lot of efficient blue emitters with TADF characteristics were developed<sup>5, 11-22, 52-53</sup>. Indeed, the diversity of TADF molecular design has made it much easier to achieve blue emission than tradition iridium or platinum complexes. In order to obtain TADF molecules with high efficiency, two key requirements have to be fulfilled simultaneously<sup>23</sup>: 1. Spatially separated HOMO (highest occupied molecular orbital) and LUMO (lowest unoccupied molecular orbital) moieties to provide a small overlap between HOMO and LUMO; 2. Strong resonance from  $S_1$  to  $S_0$  to ensure efficient radiative decay. The first requirement can be achieved simply by introducing the electron withdrawing groups and electron donating groups with a relatively large torsion angle in between<sup>24</sup>. Numerous TADF emitters bearing this concept with various electron withdrawing groups such as triazine<sup>6, 25-29</sup>, sulfones<sup>30-34</sup>, cyanobenzenes<sup>35-40</sup>, boron<sup>14, 41-46</sup>, etc. have been reported.

Trifluoromethyl ( $-CF_3$ ) is an interesting electron-withdrawing group and has been mostly employed in phosphorescent materials to increase the electron-transporting ability and decrease molecule stacking<sup>47</sup>. However, only few molecules with  $-CF_3$  as electron-withdrawing groups have been reported for TADF materials<sup>48</sup>. In an aim to expand the diversity of TADF species and produce more potential deep blue emitters, we designed a series of TADF molecules with  $-CF_3$  substituted phenyl or pyridine rings as electron-withdrawing units and carbazole-phenyl as electron-donating unit. The different substitution position of  $-CF_3$  groups can yield various emitters with significantly diversified photophysical, electrochemical and thermal properties, etc. Additionally, we exploited the potential of these deep blue emitters as hosts for iridium complex, which could further promote the application of TADF emitters in OLED design and fabrication.

<sup>a</sup> Institute of Advanced Materials (IAM), Nanjing Tech University, Nanjing, 210023, P. R. China. E-mail: iamheng@njtech.edu.cn.

<sup>b</sup> State Key Laboratory of Coordination Chemistry, Collaborative Innovation Center of Advanced Microstructures, Jiangsu Key Laboratory of Advanced Organic Materials, School of Chemistry and Chemical Engineering, Nanjing University, Nanjing, 210023, P. R. China. E-mail: yxzheng@nju.edu.cn.

† Electronic Supplementary Information (ESI) available: CV, TGA, DTA, <sup>1</sup>H NMR and <sup>13</sup>C NMR, absolute quantum yield. See DOI: 10.1039/x0xx00000x



**Scheme 1:** Synthetic procedures of four trifluoromethyl based compounds.

## Results and discussion

### Synthesis of four compounds

All four trifluoromethyl based compounds were synthesized through Suzuki coupling reaction using Pd(PPh<sub>3</sub>)<sub>4</sub> as catalyst (Scheme 1). **TN3T-PCZ**, **TN4T-PCZ** and **DTF-PCZ** were obtained by direct coupling of corresponding boronic acid derivatives and 9-(4-bromophenyl)-9H-carbazole, while **NTN-PCZ** was synthesized from coupling reaction of (4-(9H-carbazol-9-yl)phenyl)boronic acid and 5-bromo-2-(trifluoromethyl)pyrimidine. Compounds **1** and **2** were prepared according to our previous work<sup>49</sup>. All compounds were comprehensively characterized and detailed information can be found in *cf.* Experimental Section.

### Photophysical property

Photophysical properties of four compounds were investigated by UV-vis absorption and photoluminescence spectra at room temperature, as depicted in Fig. 1 and Table 1. The maximum emission wavelengths in toluene solutions are 387, 406, 428, 411 nm for **DTF-PCZ**, **NTN-PCZ**, **TN3T-PCZ**, **TN4T-PCZ**, respectively. All compounds exhibit strong emission in deep blue region or even ultraviolet region. To our best knowledge, these emitters are among the bluest in TADF based device criterion<sup>50</sup>. The energy gaps between HOMO and LUMO of these materials were determined by calculating from the red-edge onset of UV absorption spectra, which correlate well with the trend of corresponding photoluminescence spectra. Compounds **TN3T-PCZ** and **TN4T-PCZ** have quite different emission profiles despite the similarities in terms of molecular structures due to the increased steric hindrance from -CF<sub>3</sub> units in **TN3T-PCZ** and also the HOMO/LUMO distribution patterns that are simultaneously affected by the position of -CF<sub>3</sub> groups and pyridine rings. The absolute photoluminescence quantum yields of all compounds are determined on a Horiba FL-3

spectrometer in degassed toluene solutions with an integer sphere. All deep blue emitters show decent quantum yields (71.84-86.93%) (Table 1) and could be potentially solid blue emitter candidates for OLED application.

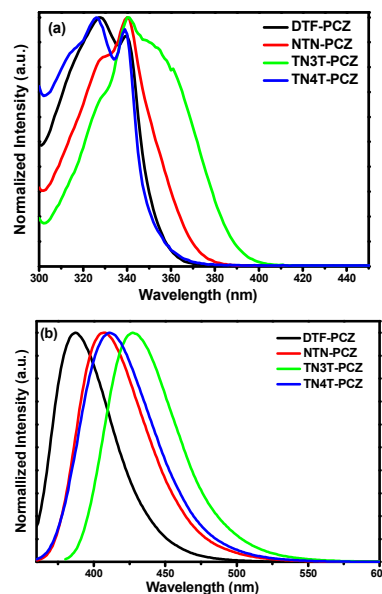


**Fig. 1** (a) Normalized absorption and (b) photoluminescence spectra in degassed toluene solution ( $5 \times 10^{-5}$  M) at 300 K.

**Table 1.** Photophysical and electrochemical properties of four compounds

Compounds	UV/ $\lambda_{\max}$ <sup>[a]</sup> (nm)	$E_g$ <sup>[b]</sup> (eV)	PL/ $\lambda_{\max}$ <sup>[c]</sup> (nm)	$\varphi_{\text{abs}}$ <sup>[d]</sup> (%)	FWHM <sup>[e]</sup> (nm)	HOMO <sup>[f]</sup> /LUMO <sup>[g]</sup> (eV)	$T_g$ <sup>[h]</sup> / $T_d$ <sup>[i]</sup> (°C)	CIE <sub>x,y</sub> <sup>[j]</sup>	$\Delta E_{\text{ST}}$ <sup>[k]</sup> (eV)
<b>DTF-PCZ</b>	327,339	3.37	387	75.98	49	-5.73/-2.36	185/221	(0.16,0.02)	0.07
<b>NTN-PCZ</b>	328,339	3.25	406	74.16	56	-5.76/-2.51	-/241	(0.16,0.03)	0.12
<b>TN3T-PCZ</b>	327,340,348	3.13	428	71.84	57	-5.74/-2.61	282/265	(0.15,0.05)	0.09
<b>TN4T-PCZ</b>	326,338	3.20	411	86.93	59	-5.76/-2.56	207/246	(0.15,0.03)	0.10

[a] Maximum absorption wavelength in toluene solution ( $5 \times 10^{-5}$  M); [b] Band gap energies calculated from onset of UV spectrum using  $E_g = hc/\lambda$ ; [c] Maximum photoluminescence wavelength in toluene solution ( $5 \times 10^{-5}$  M); [d] Absolute photoluminescence quantum yield in degassed toluene solution; [e] Full width at half maxima of photoluminescence spectrum; [f] HOMO energy level calculated from oxidation potentials from cyclic voltammetry using ferrocene as standard; [g] LUMO energy level determined by HOMO and  $E_g$ ; [h] Glass transition temperature from DSC; [i] Decomposition temperature from TGA corresponds to 5% weight loss. [j] CIE coordinates of corresponding photoluminescence spectrum in toluene; [k] Energy gap between  $S_1$  and  $T_1$  from onset of fluorescence and phosphorescence at 77 K in toluene, Fig. S5-Fig. S8 (ESI†).

### Theoretical Calculation

To gain insight into the transitional properties and understand the detail of HOMO/LUMO distributions, theoretical calculations based on density functional theory (DFT) with B3LYP (6-31g) basis set were performed on these emitters. As illustrated in Fig. 2, HOMO and LUMO moieties are all sufficiently separated, which contribute to the small  $\Delta E_{\text{ST}}$ . The HOMO moieties are mostly localized on carbazole fragments and phenyl-bridges, wherein LUMO moieties are mainly localized on phenyl/pyridine-rings substituted by  $-\text{CF}_3$  groups. A small portion of overlap can be observed at phenyl-bridge between the electron donor and acceptor units, which not only creates a reasonable torsion angle ( $\alpha$ ), *c.f.* Table S5 (ESI†) to decrease the energy gap between  $S_1$  and  $S_0$ , but also facilitate the subsequent radiative decay. **TN3T-PCZ** differs from other three molecules with a much larger torsion angle between electron acceptor unit and phenyl-bridge, leading to a weaker oscillating strength, as demonstrated in Table S5 (ESI†), and also a relatively lower photoluminescence quantum yield.

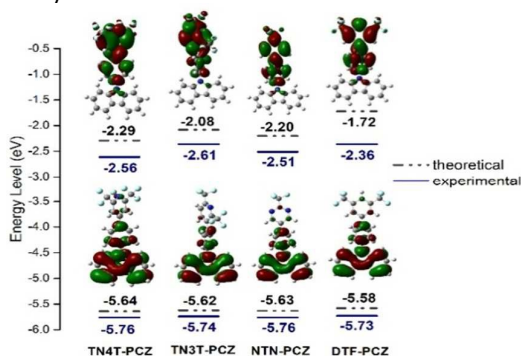


**Fig. 2** HOMO and LUMO energy level diagram and distributions of four molecules.

### Thermal stability

Thermogravimetric analysis (TGA) and differential scanning calorimetry (DSC) curves at a heating rate of  $10^\circ\text{C}/\text{min}$  were conducted on these compounds to investigate their thermal stability. All compounds exhibit moderate stability with decomposition temperatures higher than  $220^\circ\text{C}$ . **TN4T-PCZ** has the highest  $T_d$ , and even though compounds **TN3T-PCZ** and **TN4T-PCZ** have the same molecule weight, their thermal stability is quite different from each other. The above mentioned torsion angle  $\alpha$  could be attributed to such difference in terms of thermal stability, and further affect the overall OLED performances. Nevertheless, it is still adequate for OLED fabrication utilizing these four compounds as guests in emitting layer and also feasible for applications as hosts for other emitters.

### Electroluminescence properties

Since all four compounds exhibit strong emission in deep blue region with large energy gap between HOMO and LUMO energy levels, they can not only be anticipated as strong candidates as emitters in OLED emission layer, but also sufficiently as hosts for tradition phosphorescent emitters, such as iridium complexes. To further evaluate their electroluminescence properties, two types of devices with configurations as follows were fabricated: Device type 1:  $\text{MoO}_3$  / TAPC (di-[4-(*N,N*-ditolyl-amino)-phenyl] cyclohexane) / 2,6-DCzppy (2,6-bis(3-(9*H*-carbazol-9-yl)phenyl) pyridine) : x wt% guest / TmPyPB (1,3,5-tri[(3-pyridyl)-phen-3-yl]benzene) / LiF/Al; Device type 2)  $\text{MoO}_3$ /TAPC/ Host : x wt% iridium complex /TmPyPB/LiF/Al. The schematic energy diagram of each configuration can be found in Fig. 3a and 3b. In all device configurations, we employed  $\text{MoO}_3$  as hole injecting layer (HIL), TAPC as hole-transporting layer (HTL), TmPyPB as electron-transporting layer (ETL), LiF as electron injecting layer (EIL). For the device type 1, 2, 6-DCzppy was employed as the host, **TN4T-PCZ** or **NTN-PCZ** was the guest. The optimal device configurations of two compounds are  $\text{MoO}_3$  (2 nm)/TAPC(7 nm)/(2,6-DCzppy: 6 wt% **NTN-PCZ**) (10 nm)/ TmPyPB (15 nm)

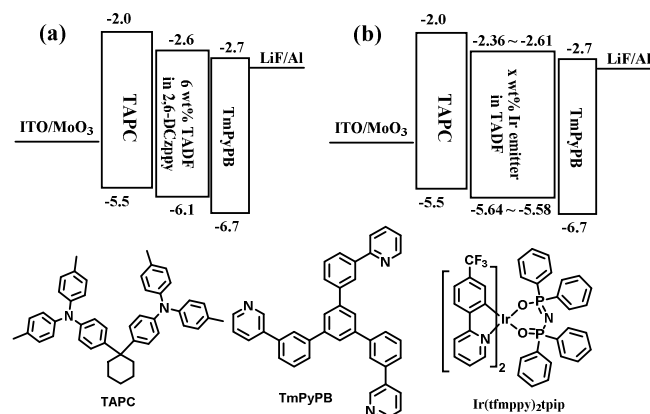


**Fig. 3** (a) Device structure energy diagram for type 1; (b) Device structure energy diagram for type 2 and materials employed in two types of devices.

and MoO<sub>3</sub> (2 nm)/ TAPC (15 nm) / (2,6-DCzppy: 6 wt% **TN4T-PCZ**) (5 nm)/ TmPyPB (30 nm) for **NTN-PCZ** and **TN4T-PCZ**, respectively. In device type 2 configuration, four compounds are employed as hosts for a green phosphorescent emitter **Ir(tfmpppy)<sub>2</sub>tpip** (tfmpppy= 2-(4-(trifluoromethyl)phenyl)pyridine, tpip= *N*-(diphenylphosphoryl)-*P,P*-diphenylphosphinic amide)<sup>49</sup>, which is an efficient green emitter previously reported in our group<sup>47</sup>. The general thickness of each layer is almost identical for all four compounds except for the doping concentrations of **Ir(tfmpppy)<sub>2</sub>tpip**, *c.f.* Fig. 3. The optimized device configurations are MoO<sub>3</sub> (2 nm) /TAPC (30 nm)/ (Host: x wt% iridium complex) (10 nm)/ TmPyPB (30 nm)/ LiF/ Al, with 6 wt% iridium complex for **TN3T-PCZ**, **NTN-PCZ**, **DTF-PCZ** and 16 wt%

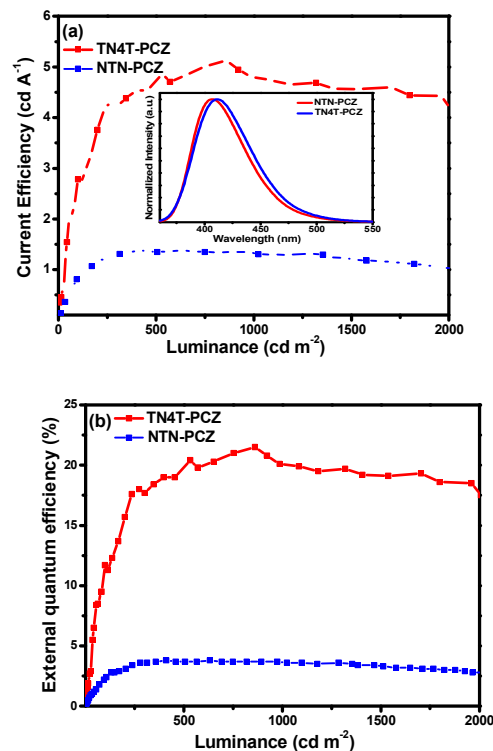


**Fig. 4** (a) Luminance-voltage and (b) current efficiency-luminance curves for type 1 devices.

for **TN4T-PCZ**, respectively.

In device type 1, both devices based on **NTN-PCZ** and **TN4T-PCZ** exhibit efficient energy transfer from 2,6-DCzppy host to the emitters. However, as shown in Fig. 4 Fig. S17 and Table 2,

**Table 2.** Electroluminescence performances of two types of devices.

Device Type	$V_{\text{turn-on}}$ <sup>[a]</sup> (V)	$L_{\text{max}}$ <sup>[b]</sup> (cd m <sup>-2</sup> )	$\eta_{\text{c,max}}$ <sup>[c]</sup> (cd A <sup>-1</sup> )	$\eta_{\text{c}}$ at 100 cd m <sup>-2</sup> <sup>[d]</sup> (cd A <sup>-1</sup> )	$\eta_{\text{c}}$ at 1000 cd m <sup>-2</sup> <sup>[e]</sup> (cd A <sup>-1</sup> )	CIE <sup>[f]</sup> (x,y)	EQE <sub>max</sub> <sup>[g]</sup> (%)
Type 1: <b>NTN-PCZ</b>	4.1 V	2337	1.38	0.87	1.30	(0.17,0.06)	3.8
Type 1: <b>TN4T-PCZ</b>	4.2 V	5377	5.01	2.69	4.74	(0.16,0.03)	20.4
Type 2: <b>DTF-PCZ</b>	4.5 V	23263	53.01	36.33	32.14	(0.30,0.64)	13.7
Type 2: <b>NTN-PCZ</b>	3.9 V	11265	54.61	30.33	21.52	(0.30,0.64)	14.1
Type 2: <b>TN3T-PCZ</b>	4.9 V	14270	57.00	53.79	34.62	(0.30,0.64)	18.6
Type 2: <b>TN4T-PCZ</b>	6.4 V	18171	66.56	24.61	19.93	(0.29,0.62)	17.5

[a] turn-on voltage; [b] maximum brightness; [c] maximum current efficiency; [d] current efficiency at the brightness of 100 cd m<sup>-2</sup>; [e] current efficiency at the brightness of 1000 cd m<sup>-2</sup>; [f] CIE coordinates of electroluminescence spectrum; [g] maximum external efficiency.

## Paper

## NJC

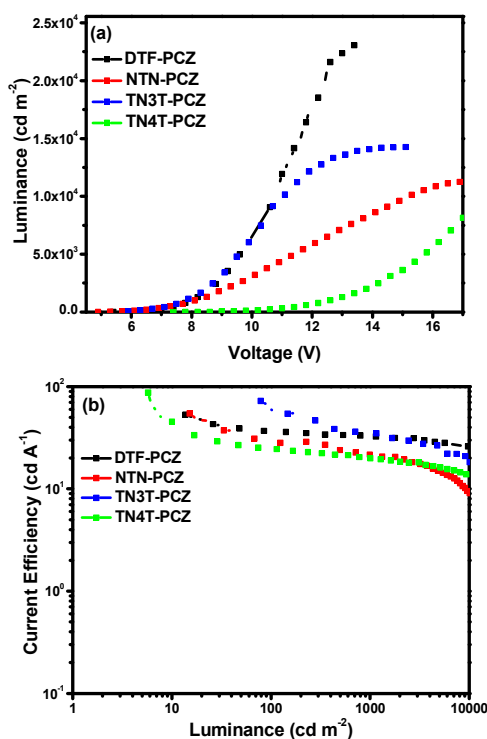


**Fig. 5** (a) Luminance-voltage and (b) current efficiency-luminance curves for type 2 devices.

device based on **TN4T-PCZ** shows superior performance compared to the device based on **NTN-PCZ**. The maximum brightness for device based on **TN4T-PCZ** is  $5377 \text{ cd m}^{-2}$ . Though the current efficiency is only  $5.01 \text{ cd A}^{-1}$ , the external quantum efficiency of this device can reach 20.4% because a large portion of the emission spectrum covers the ultraviolet region, which cannot be detected by the photomultiplier used in our laboratory. These results are remarkable in deep blue TADF category<sup>24</sup>. The electroluminescence spectrum also correlates well with the emission spectrum in toluene solution. Both devices show moderate turn-on voltages, and relatively small efficiency roll-off.

The employment of TADF materials as hosts for phosphorescent emitters can help dilute the density of triplet excitons and increase the rate of exciton utilization<sup>51</sup>. The high-lying triplet state of TADF materials can also help reduce the reverse energy transfer from guest to host<sup>50</sup>. On the basis of these reasons, we further exploited the potential of using these TADF materials as hosts for iridium complexes. All devices show decent overall performance. For devices utilizing **DTF-PCZ** and **NTN-PCZ** as hosts, the turn-on voltages are relatively lower than the other two candidates (Table 2), which could originate from the smaller energy barrier between LUMOs of hosts and ETL, resulting in much easier electron injection and transportation. Device with **DTF-PCZ** as host exhibits the highest brightness of  $23263 \text{ cd m}^{-2}$  and smallest efficiency roll off even though the external quantum efficiency are the lowest in all four devices as revealed in Fig. 5, Table 2

and Fig.S16 (ESI<sup>†</sup>). **TN3T-PCZ** serves as a suitable host for **Ir(fmppy)<sub>2</sub>tppip** since the corresponding device has a relatively lower turn-on voltage and the highest external quantum efficiency of 18.6%. It is also worth mentioning that the doping concentration for device with **TN4T-PCZ** as host is surprisingly high, it requires 16 wt% of guest emitter to ensure the energy transfer from host to guest, but the energy conversion is still insufficient in the case of **TN4T-PCZ** and a small portion of emission from **TN4T-PCZ** can still be observed in the electroluminescence spectrum, Fig. S16 (ESI<sup>†</sup>). This can be rationalized by the strong oscillating strength ( $f$ ) between  $S_1$  and  $S_0$ , which promote the subsequent radiative decay of **TN4T-PCZ** instead rather than energy transfer to guest emitter. This could also explain the higher turn-on voltage of 6 V, and indicating **TN4T-PCZ** as a less proper candidate for application as host in OLED structure.

## Conclusions

Four trifluoromethyl based TADF emitters **DTF-PCZ**, **NTN-PCZ**, **TN3T-PCZ**, **TN4T-PCZ** exhibit strong deep blue emission and are among the bluest emitters in TADF category. When used as blue emitter in pragmatic OLED applications, device based on **TN4T-PCZ** has significantly high external quantum efficiency up to 20.4% with moderate efficiency roll-off. These TADF materials can also serve as hosts for phosphorescent emitters. High external quantum efficiency and small efficiency roll off can be attained utilizing an efficient green iridium complex doped in these trifluoromethyl based TADF compounds. Especially, device with **TN3T-PCZ** as host yields a maximum brightness of  $23267 \text{ cd m}^{-2}$  and a maximum external quantum efficiency of 18.6% with relatively small efficiency roll-off. Even though the overall performances of these devices are still inferior to the conventional bipolar hosts, the strategy of introducing TADF molecules as host and guest can still be a useful alternative for OLED application.

## Experimental section

### Synthetic procedures and characterization

**Synthesis of (2,6-bis(trifluoromethyl)pyridin-3-yl)boronic acid (1) and (2,6-bis(trifluoromethyl)pyridin-4-yl) boronic acid (2).** To a solution of 2,6-bis(trifluoromethyl) pyridine (2.15 g, 10 mmol) in 50 ml anhydrous ether was added LDA (1.5 M, 10 mmol) at  $-78^\circ\text{C}$  in  $\text{N}_2$  atmosphere under stirring for 1 h before the addition of triisopropyl borate (2.26 g, 12 mmol). The reaction mixture was then slowly warmed to room temperature and the resulting solution was then added 2 M NaOH until the pH value reached 10 and the organic phase was discarded. The resulting water solution was then added 2 M HCl until the pH of the solution reached 6 and extracted with 20 ml ether for three times. The organic phase was then combined and solvent was removed under reduced pressure, giving a light-brownish liquid (1.03 g, 40%) which was the mixture of 1 and 2. To reduce the loss on column chromatography, the mixture was directly put into next step without further purification.

**Synthesis of TN3T-PCZ, TN4T-PCZ.** The mixture of 2.58 g (10 mmol) (2,6-bis(trifluoromethyl)pyridin-3-yl)boronic acid (1) with (2,6-bis(trifluoromethyl)pyridin-4-yl)boronic acid (2) and 9-(4-bromophenyl)-9H-carbazole (3.86 g, 12 mmol),  $K_2CO_3$  (1.38 g, 10 mmol),  $Pd(PPh_3)_4$  (0.35 g, 0.3 mmol) in a bottle was degassed and filled with  $N_2$ , then 50 ml THF :  $H_2O$  = 1 : 1 was added. The reaction mixture was refluxed for 24 h. After cooling to room temperature, the solvent was removed and purified through column chromatography with petroleum ether: ethyl acetate = 10 : 1 as eluent, yielding **TN3T-PCZ** (1.59 g, 35%) and **TN4T-PCZ** (1.92 g, 42%) as white powders. Then they were purified again through sublimation prior to device fabrication. **TN3T-PCZ**:  $^1H$  NMR( $CDCl_3$ , 400 MHz)  $\delta$  8.17 (d,  $J$  = 7.3 Hz, 4H), 8.00 – 7.91 (m, 2H), 7.86 – 7.77 (m, 2H), 7.53 – 7.40 (m, 4H), 7.34 (ddd,  $J$  = 8.0, 6.8, 1.4 Hz, 2H);  $^{13}C$  NMR( $CDCl_3$ , 101 MHz):  $\delta$  151.54, 149.77, 149.42, 140.34, 140.27, 134.26, 128.84, 127.86, 126.23, 123.80, 122.30, 120.81, 120.61, 120.54, 119.56, 109.60; Elemental Analysis: calculated: C: 65.79, H: 3.09; N: 6.14; experimental: C: 65.70; H: 3.10; N: 6.21; ESI-MS: calculated: 456.39, [M+1]: 457.18. **TN4T-PCZ**:  $^1H$  NMR( $CDCl_3$ , 400 MHz)  $\delta$  8.17 (dt,  $J$  = 7.6, 0.9 Hz, 2H), 8.07 (d,  $J$  = 8.0 Hz, 1H), 7.99 (d,  $J$  = 8.0 Hz, 1H), 7.76 – 7.67 (m, 2H), 7.62 – 7.55 (m, 2H), 7.53 – 7.41 (m, 4H), 7.33 (ddd,  $J$  = 8.1, 6.9, 1.3 Hz, 2H);  $^{13}C$  NMR( $CDCl_3$ , 101 MHz)  $\delta$  141.95, 140.55, 138.63, 134.60, 130.21, 126.85, 126.12, 123.64, 122.74, 120.45, 120.36, 109.67, 95.98; Elemental Analysis: calculated: C: 65.79, H: 3.09; N: 6.14; experimental: C: 65.89, H: 3.17; N: 6.14; ESI-MS: calculated: 456.39, [M+1]: 457.30.

**Synthesis of DTF-PCZ.** A mixture of (3,5-bis(trifluoromethyl)phenyl)-boronic acid (2.58 g, 10 mmol) and 9-(4-bromophenyl)-9H-carbazole (3.86 g, 12 mmol),  $K_2CO_3$  (1.38 g, 10 mmol),  $Pd(PPh_3)_4$  (0.35 g, 0.3 mmol) was dissolved in 50 ml THF :  $H_2O$  = 1 : 1 and refluxed for 24 h before cool down to room temperature. The resulting mixture was dealt similar to the above mentioned process and purified through column chromatography to yield 3.87 g (85%) product as white powder. **DTF-PCZ**:  $^1H$  NMR( $CDCl_3$ , 400 MHz)  $\delta$  8.17 (dt,  $J$  = 7.6, 0.9 Hz, 2H), 8.07 (d,  $J$  = 8.0 Hz, 1H), 7.99 (d,  $J$  = 8.0 Hz, 1H), 7.76 – 7.67 (m, 2H), 7.62 – 7.55 (m, 2H), 7.53 – 7.41 (m, 4H), 7.33 (ddd,  $J$  = 8.1, 6.9, 1.3 Hz, 3H);  $^{13}C$  NMR( $CDCl_3$ , 101 MHz)  $\delta$  141.95, 140.55, 138.63, 134.60, 130.21, 126.85, 126.12, 123.64, 122.74, 120.45, 120.36, 109.67, 95.98; Elemental Analysis: calculated: C: 68.57, H: 3.32; N: 3.08; experimental: C: 68.65; H: 3.30; N: 3.05; ESI-MS: calculated: 455.40, [M+1]: 456.52.

**Synthesis of NTN-PCZ.** A mixture of (4-(9H-carbazol-9-yl)phenyl)-boronic acid (3.44 g, 12 mmol) and 5-bromo-2-(trifluoromethyl)pyrimidine (2.27 g, 10 mmol),  $K_2CO_3$  (1.38 g, 10 mmol),  $Pd(PPh_3)_4$  (0.35 g, 0.3 mmol) was dissolved in 50 ml THF :  $H_2O$  = 1 : 1 and refluxed for 24 h and processed similar to abovementioned procedure. The final product was purified through column chromatography to yield 3.54 g (91%) **NTN-PCZ** as white powder. **NTN-PCZ**:  $^1H$  NMR ( $CDCl_3$ , 400 MHz)  $\delta$  9.21 (s, 2H), 8.17 (dt,  $J$  = 7.7, 0.9 Hz, 2H), 7.91 – 7.78 (m, 4H), 7.53 – 7.40 (m, 4H), 7.33 (ddd,  $J$  = 8.0, 6.9, 1.3 Hz, 2H);  $^{13}C$  NMR ( $CDCl_3$ , 101 MHz)  $\delta$  155.73, 155.43, 140.41, 139.58, 135.36, 131.57, 128.81, 128.03, 126.20, 123.74, 121.06, 120.54, 120.51, 118.32, 109.60, 77.33, 77.22, 77.02, 76.70; Elemental Analysis: calculated: C: 70.95, H: 3.62; N: 10.78; experimental: C: 70.89; H: 3.67; N: 10.79; ESI-MS: calculated: 389.38, [M+1]: 390.54.

## Conflicts of interest

There are no conflicts to declare.

## Acknowledgements

This work is supported by National Natural Science Foundation of China (21402088, 51773088) and the Natural Science Foundation of Jiangsu Province (BY2016075-02).

## Notes and references

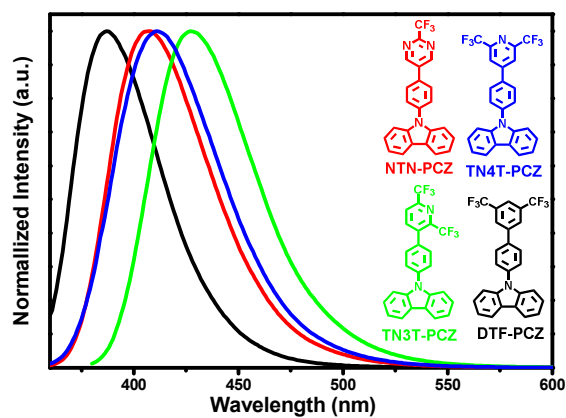
- C. W. Tang and S. A. VanSlyke, *Appl. Phys. Lett.*, 1987, **51**, 913-915.
- Y. Tao, K. Yuan, T. Chen, P. Xu, H. Li, R. Chen, C. Zheng, L. Zhang and W. Huang, *Adv. Mater.*, 2014, **26**, 7931-7958.
- C. Adachi, M. A. Baldo, M. E. Thompson and S. R. Forrest, *J. Appl. Phys.*, 2001, **90**, 5048-5051.
- D. F. O. B. M. A. Baldo, Y. You, A. Shoustikov, S. Sibley, M. E. Thompson, S. R. Forrest, *Nature*, 1998, 151-154.
- H. Nakanotani, T. Higuchi, T. Furukawa, K. Masui, K. Morimoto, M. Numata, H. Tanaka, Y. Sagara, T. Yasuda and C. Adachi, *Nat. Commun.*, 2014, **5**, 4016.
- H. Tanaka, K. Shizu, H. Miyazaki and C. Adachi, *Chem. Commun.*, 2012, **48**, 11392-11394.
- T. Nakagawa, S. Y. Ku, K. T. Wong and C. Adachi, *Chem. Commun.*, 2012, **48**, 9580-9582.
- G. Mehes, H. Nomura, Q. Zhang, T. Nakagawa and C. Adachi, *Angew. Chem. Int. Ed.*, 2012, **51**, 11311-11315.
- K. Goushi, K. Yoshida, K. Sato and C. Adachi, *Nat. Photonics*, 2012, **6**, 253-258.
- H. Uoyama, K. Goushi, K. Shizu, H. Nomura and C. Adachi, *Nature*, 2012, **492**, 234-238.
- L. S. Cui, H. Nomura, Y. Geng, J. U. Kim, H. Nakanotani and C. Adachi, *Angew. Chem. Int. Ed.*, 2017, **56**, 1571-1575.
- H. Shin, J. H. Lee, C. K. Moon, J. S. Huh, B. Sim and J. J. Kim, *Adv. Mater.*, 2016, **28**, 4920-4925.
- M. Kim, S. K. Jeon, S. H. Hwang, S. S. Lee, E. Yu and J. Y. Lee, *Chem. Commun.*, 2016, **52**, 339-342.
- T. Hatakeyama, K. Shiren, K. Nakajima, S. Nomura, S. Nakatsuka, K. Kinoshita, J. Ni, Y. Ono and T. Ikuta, *Adv. Mater.*, 2016, **28**, 2777-2781.
- Q. Zhang, D. Tsang, H. Kuwabara, Y. Hatae, B. Li, T. Takahashi, S. Y. Lee, T. Yasuda and C. Adachi, *Adv. Mater.*, 2015, **27**, 2096-2100.
- D. R. Lee, M. Kim, S. K. Jeon, S. H. Hwang, C. W. Lee and J. Y. Lee, *Adv. Mater.*, 2015, **27**, 5861-5867.
- H. Kaji, H. Suzuki, T. Fukushima, K. Shizu, K. Suzuki, S. Kubo, T. Komino, H. Oiwa, F. Suzuki, A. Wakamiya, Y. Murata and C. Adachi, *Nat. Commun.*, 2015, **6**, 8476.
- Y. J. Cho, B. D. Chin, S. K. Jeon and J. Y. Lee, *Adv. Funct. Mater.*, 2015, **25**, 6786-6792.
- Y. J. Cho, K. S. Yook and J. Y. Lee, *Adv. Mater.*, 2014, **26**, 4050-4055.
- F. B. Dias, K. N. Bourdakos, V. Jankus, K. C. Moss, K. T. Kamtekar, V. Bhalla, J. Santos, M. R. Bryce and A. P. Monkman, *Adv. Mater.*, 2013, **25**, 3707-3714.
- Q. Zhang, J. Li, K. Shizu, S. Huang, S. Hirata, H. Miyazaki and C. Adachi, *J. Am. Chem. Soc.*, 2012, **134**, 14706-14709.
- S. Youn Lee, T. Yasuda, H. Nomura and C. Adachi, *Appl. Phys. Lett.*, 2012, **101**, 093306.

## NJC

## Paper

23. M. K. Etherington, J. Gibson, H. F. Higginbotham, T. J. Penfold and A. P. Monkman, *Nat. Commun.*, 2016, **7**, 13680.
24. M. Y. Wong and E. Zysman-Colman, *Adv. Mater.*, 2017, **29**, 160544
25. Y. Xiang, S. Gong, Y. Zhao, X. Yin, J. Luo, K. Wu, Z.-H. Lu and C. Yang, *J. Mater. Chem. C*, 2016, **4**, 9998-10004.
26. W. Y. Hung, P. Y. Chiang, S. W. Lin, W. C. Tang, Y. T. Chen, S. H. Liu, P. T. Chou, Y. T. Hung and K. T. Wong, *ACS Appl. Mater. Interfaces*, 2016, **8**, 4811-4818.
27. J.-R. Cha, C. W. Lee, J. Y. Lee and M.-S. Gong, *Dyes Pigments*, 2016, **134**, 562-568.
28. H. Tanaka, K. Shizu, H. Nakanotani and C. Adachi, *J. Phys. Chem. C* 2014, **118**, 15985-15994.
29. T. Serevicius, T. Nakagawa, M. C. Kuo, S. H. Cheng, K. T. Wong, C. H. Chang, R. C. Kwong, S. Xia and C. Adachi, *Phys. Chem. Chem. Phys.*, 2013, **15**, 15850-15855.
30. J. W. Yang, J. M. Choi and J. Y. Lee, *Phys. Chem. Chem. Phys.*, 2016, **18**, 31330-31336.
31. C. Fan, C. Duan, C. Han, B. Han and H. Xu, *ACS Appl. Mater. Interfaces*, 2016, **8**, 27383-27393.
32. M. Liu, Y. Seino, D. Chen, S. Inomata, S. J. Su, H. Sasabe and J. Kido, *Chem. Commun.*, 2015, **51**, 16353-16356.
33. S. H. Wu, M. Aonuma, Q. S. Zhang, S. P. Huang, T. Nakagawa, K. Kuwabara and C. Adachi, *J. Mater. Chem. C* 2014, **2**, 421-424.
34. H. Wang, L. Xie, Q. Peng, L. Meng, Y. Wang, Y. Yi and P. Wang, *Adv. Mater.*, 2014, **26**, 5198-5204.
35. S. Wang, Z. Cheng, X. Song, X. Yan, K. Ye, Y. Liu, G. Yang and Y. Wang, *ACS Appl. Mater. Interfaces*, 2017, **9**, 9892-9901
36. X. Cao, J. Hu, Y. Tao, W. Yuan, J. Jin, X. Ma, X. Zhang and W. Huang, *Dyes & Pigments*, 2017, **136**, 543-552.
37. J. Zhang, J. Li, W. H. Chen, D. Zheng, J. S. Yu, H. Wang and B. S. Xu, *Tetrahedron Lett.*, 2016, **57**, 2044-2048.
38. I. S. Park, S. Y. Lee, C. Adachi and T. Yasuda, *Adv. Funct. Mater.*, 2016, **26**, 1813-1821.
39. H. Noda, R. Kabe and C. Adachi, *Chem. Lett.*, 2016, **45**, 1463-1466.
40. B. Li, H. Nomura, H. Miyazaki, Q. Zhang, K. Yoshida, Y. Suzuma, A. Orita, J. Otera and C. Adachi, *Chem. Lett.*, 2014, **43**, 319-321.
41. P. Stachelek, A. A. Alsimaree, R. B. Alnoman, A. Harriman and J. G. Knight, *J. Phys. Chem. A* 2017, **121**, 2096-2107.
42. Y.-J. Shiu, Y.-T. Chen, W.-K. Lee, C.-C. Wu, T.-C. Lin, S.-H. Liu, P.-T. Chou, C.-W. Lu, I. C. Cheng, Y.-J. Lien and Y. Chi, *J. Mater. Chem. C* 2017, **5**, 1452-1462.
43. Y. J. Shiu, Y. C. Cheng, W. L. Tsai, C. C. Wu, C. T. Chao, C. W. Lu, Y. Chi, Y. T. Chen, S. H. Liu and P. T. Chou, *Angew. Chem. Int. Ed.*, 2016, **55**, 3017-3021.
44. M. L. Daly, C. A. DeRosa, C. Kerr, W. A. Morris and C. L. Fraser, *RSC Adv.*, 2016, **6**, 81631-81635.
45. K. Suzuki, S. Kubo, K. Shizu, T. Fukushima, A. Wakamiya, Y. Murata, C. Adachi and H. Kaji, *Angew. Chem. Int. Ed.*, 2015, **54**, 15231-15235.
46. H. Hirai, K. Nakajima, S. Nakatsuka, K. Shiren, J. Ni, S. Nomura, T. Ikuta and T. Hatakeyama, *Angew. Chem. Int. Ed.*, 2015, **54**, 13581-13585.
47. Y. C. Zhu, L. Zhou, H. Y. Li, Q. L. Xu, M. Y. Teng, Y. X. Zheng, J. L. Zuo, H. J. Zhang and X. Z. You, *Adv. Mater.*, 2011, **23**, 4041-4046.
48. L. Mei, J. Hu, X. Cao, F. Wang, C. Zheng, Y. Tao, X. Zhang and W. Huang, *Chem. Commun.*, 2015, **51**, 13024-13027.
49. Q.-L. Xu, X. Liang, S. Zhang, Y.-M. Jing, X. Liu, G.-Z. Lu, Y.-X. Zheng and J.-L. Zuo, *J. Mater. Chem. C* 2015, **3**, 3694-3701.
50. M. Godumala, S. Choi, M. J. Cho and D. H. Choi, *J. Mater. Chem. C* 2016, **4**, 11355-11381.
51. X. Y. Liu, F. Liang, Y. Yuan, L. S. Cui, Z. Q. Jiang and L. S. Liao, *Chem. Commun.*, 2016, **52**, 8149-8151.
52. J. W. Sun, J. Y. Baek, K. H. Kim, C. K. Moon, J. H. Lee, S. K. Kwon, Y. H. Kim and J. J. Kim, *Chem. Mater.*, 2015, **27**, 6675.
53. J. W. Sun, J. Y. Baek, K. H. Kim, J. S. Huh, S. K. Kwon, T. H. Kim and J. J. Kim, *J. Mater. Chem. C* 2017, **5**, 1027.

## Graphical abstract



Four deep blue TADF compounds with trifluoromethyl-substituted phenyl/*N*-heterocyclic rings were investigated both as hosts and guests in decent OLEDs.